Available online at www.sciencedirect.com
ScienceDirect
Polymer 48 (2007) 4601–4608
polymer
www.elsevier.com/locate/polymer

Theoretical study on morphology of ABCD 4-miktoarm star block copolymer

Rong Wang*, Tingting Xu

Department of Polymer Science and Engineering, School of Chemistry and Chemical Engineering, Nanjing University, Nanjing 210093, China

Received 5 May 2007; received in revised form 15 May 2007; accepted 16 May 2007
Available online 25 May 2007

Abstract

A real-space implementation of the self-consistent field theory (SCFT) has been used to study the morphologies of ABCD 4-miktoarm star block copolymers. For the sake of numerical tractability, the morphologies and the phase diagrams of ABCD 4-miktoarm star block copolymers are investigated in two dimensions (2D) by varying the volume fractions of the blocks and the interaction parameters. Many interesting and complex morphologies occur and compared with ABCD linear block copolymers; ABCD 4-miktoarm star block copolymers have more regular disciplines. We found that systems with similar components have similar morphologies and at the weaker segregation, the minority components always cannot separate from the other blocks and they easily dissolve to form one phase with other block(s), but with the increase of the segregation degree (large $\tilde{\chi}$), the ordered phases can be well separated. With the help of our computational prediction, experimental researchers can work more purposefully and efficiently.

Keywords: ABCD star block copolymer; Block copolymer; Morphology

1. Introduction

As block copolymers are becoming more and more widely used, the research on them also becomes wider and deeper. The morphologies and the phase diagrams for AB diblock copolymer, linear ABC triblock copolymer, even ABC 3-miktoarm copolymer are intensively studied both theoretically and experimentally [1–16]. The more complicated block copolymer, such as those of linear ABCA [17], and ABCD [18–22], ABCDE [20] types and even ABCD 4-miktoarm star quarterpolymer [23] (A is polystyrene, B is polybutadiene, C is polyisoprene, and D is poly(4-methylstyrene)) are synthesized. After that, Dotera et al. [24,25] found that a monodisperse symmetric ABCD star block copolymer melt undergoes a microphase separation by using Monte Carlo simulations. Among these complicated tetrablock copolymers, to our knowledge, the morphologies for the linear ABCA tetrablock terpolymer have been studied theoretically [26,27] and that the end block A is substituted by a different block D has been reported as well, that is ABCD tetrablock quarterpolymer [28]. Takano et al. [19] and Takahashi et al. [18,29] have synthesized the complex tetrablock quarterpolymer of ABCD type, and the four-phase triple coaxial cylindrical morphology and the four-phase six-layer lamellar structure were observed. Even the order-to-order (cylinder → double gyroid → lamellae) transition was observed. The above workers have done both fantastic experimental work and theoretical research for block copolymers. In order to provide the helpful ideas to design nanomaterials from these complicated block copolymers, we theoretically investigated the ABCD 4-miktomarm star block copolymer in the present work. Our calculations reasonably agree with previous theoretical and experimental results and can be used to guide the design of novel microstructures such as the fascinating star-shaped [30] and comb-shaped

* Corresponding author. Department of Polymer Science and Engineering, School of Chemistry and Chemical Engineering, Nanjing University, Room 1006, Chemistry Building, No. 22 Hankou Rd., Nanjing, Jiangsu 210093, China. Tel.: +86 25 83596802; fax: +86 25 83317761.
E-mail address: rong_wang73@hotmail.com (R. Wang).

0032-3861/$ - see front matter © 2007 Elsevier Ltd. All rights reserved.
doi:10.1016/j.polymer.2007.05.050

[31–34] copolymer systems as well as the nanomaterials. In this paper, we first present the theory of our method, then we discuss the computational results, and last we get the conclusions.

2. Self-consistent field theory and calculation algorithm

We use a combinatorial screening method based on the real-space implementation of the self-consistent field theory (SCFT), originally proposed by Drolet and Fredrickson [26,27], to search the equilibrium microphases of ABCD 4-miktoarm star block copolymer melts in this paper.

There are n ABCD 4-miktoarm star block copolymers with polymerization N in a volume V and the compositions (average volume fractions) for each block are f_A, f_B, f_C, f_D ($=1-f_A-f_B-f_C$), respectively. In the real-space SCFT one considers the statistics of a single copolymer chain in a set of effective chemical potential fields w_i, where i represents block species A, B, C or D. These chemical potential fields, which replace the actual interactions between different components, are conjugated to the segment density fields, ϕ_i, of block species i. Hence, the free energy function (in units of k_BT) of the system is given by

$$F = -\ln(Q/V) + 1/V \int \mathrm{d}\mathbf{r}[\chi_{AB}N\phi_A\phi_B + \chi_{AC}N\phi_A\phi_C + \chi_{AD}N\phi_A\phi_D + \chi_{BC}N\phi_B\phi_C + \chi_{BD}N\phi_B\phi_D + \chi_{CD}N\phi_C\phi_D - w_A\phi_A - w_B\phi_B - w_C\phi_C - w_D\phi_D - \xi(1-\phi_A-\phi_B-\phi_C-\phi_D)] \quad (1)$$

where χ_{ij} is the Flory–Huggins interaction parameter between species i and j, ξ is the Lagrange multiplier (as a pressure), $Q = \int \mathrm{d}\mathbf{r} q_i(\mathbf{r},s)q_i^+(\mathbf{r},s)$ is the partition function of a single chain in the effective chemical potential fields w_A, w_B, w_C and w_D. The end-segment distribution function $q(\mathbf{r},s)$ gives the probability that a section of a chain, of contour length s and containing a free chain end, has its "connected end" located at $\mathbf{r}$. The parameterization is chosen such that the contour variable s increases continuously from 0 to 1 corresponding from one end of the chain to the other. With the use of a flexible Gaussian chain model to describe the single-chain statistics, the functions $q_i(\mathbf{r},s)$ and $q_i^+(\mathbf{r},s)$ satisfy a modified diffusion equation.

$$\frac{\partial}{\partial s} q_i(\mathbf{r},s) = \frac{Na^2}{6}\nabla^2 q_i(\mathbf{r},s) - w_i q_i(\mathbf{r},s) \quad (2)$$

$$\frac{\partial}{\partial s} q_i^+(\mathbf{r},s) = -\frac{Na^2}{6}\nabla^2 q_i^+(\mathbf{r},s) + w_i q_i^+(\mathbf{r},s) \quad (3)$$

where $0 < s < f_iN$. And the initial conditions are $q_i(\mathbf{r},0) = \prod_{j\neq i} q_j^+(\mathbf{r},0)$ and $q_j^+(\mathbf{r},f_jN) = 1$ (i, j = A, B, C, and D). One must solve for $q_i^+(\mathbf{r},s)$ prior to solving for q_i $(\mathbf{r},s)$.

The density of each component is obtained by $\phi_i(\mathbf{r}) = V/Q\int_0^{f_i} \mathrm{d}s q_i(\mathbf{r},s)q_i^+(\mathbf{r},s)$ (i = A, B, C, and D). Minimization of the free energy to density and pressure, $\delta F/\delta\phi = \delta F/\delta\xi = 0$, leads to another five equations about the fields and the incompressibility: $w_i(\mathbf{r}) = \sum_{j\neq i}\chi_{ij}N\phi_j(\mathbf{r}) + \xi(\mathbf{r})$ and $\sum_i \phi_i(\mathbf{r}) = 1$ (i, j = A, B, C, and D).

Here we solve above equations directly in real space by using a combinatorial screening algorithm proposed by Drolet and Fredrickson [26,27]. The calculations are carried out in a two-dimensional $L_x \times L_y$ cell with periodic boundary conditions. The chain length of the polymers is fixed to be $N = 80$. The lattice spacings are chosen to be $\mathrm{d}x = \mathrm{d}y = a$, where a is the Kuhn length of the polymer segment. We choose the typical lattice sizes L_x and L_y as $\sim 10R_g$. The simulation was reiterated from 10 to 20 times or more from different initial random states to ensure that the phenomena are not accidental.

3. Results and discussions

Our focuses in the work are on the phase behaviors of ABCD 4-miktoarm star block copolymer melts in the two-dimensional demonstration. In the system there are nine tunable parameters, i.e., six interaction parameters, $\chi_{AB}N$, $\chi_{AC}N$, $\chi_{AD}N$, $\chi_{BC}N$, $\chi_{BD}N$ and $\chi_{CD}N$, and three independent compositions of components A, B and C, f_A, f_B, f_C ($f_D = 1-f_A-f_B-f_C$). Since the parameter space is so complex we mainly discuss situations under symmetrical interaction. And situations under asymmetrical interaction will also be discussed while we just consider one of them, that is we suppose $\chi_{AB}N = \chi_{CD}N = 40$, $\chi_{AC}N = \chi_{BD}N = 60$, $\chi_{AD}N = \chi_{BC}N = 20$. Of course we can assume χ_{ij} (ij = AB, BC, CD, AC, BD, AD) as any magnitude, but for the sake of computational convenience and the representativeness of the asymmetrical situation, we consider our proposal a good one.

The microphase patterns, displayed in the form of density, are the red, green, blue and white, assigned to A, B, C, and D, respectively. The final color plotted at each point is the mixture of four colors, in which the concentration of each color is proportional to the local volume fraction of an individual block.

3.1. Symmetrical interaction parameters

Due to the complicated parameter space, we first investigate the microphase-separated structures with symmetrical interaction parameters, suppose that $\chi_{AB}N = \chi_{AC}N = \chi_{AD}N = \chi_{BC}N = \chi_{BD}N = \chi_{CD}N = \tilde{\chi}$. At least 13 stable microphase-separated structures have been found as shown in Fig. 1. The morphologies and saddle-point free energies at different compositions for symmetrical interaction parameters are listed in Table 1.

When the interaction parameter is weak, such as $\tilde{\chi} = 30$, volume fractions that are close to each other cannot be easily separated, and most of the morphologies are LAM_n ($n = 2, 3$). If one of the arms, take A for example, is the small part, such as 0.1, it would be difficult to separate from other parts, instead, it will be solved in the other phase(s). And it seems that if two or three of the arms have similar proportion, they are not easy to separate either. Totally, we found eight stable

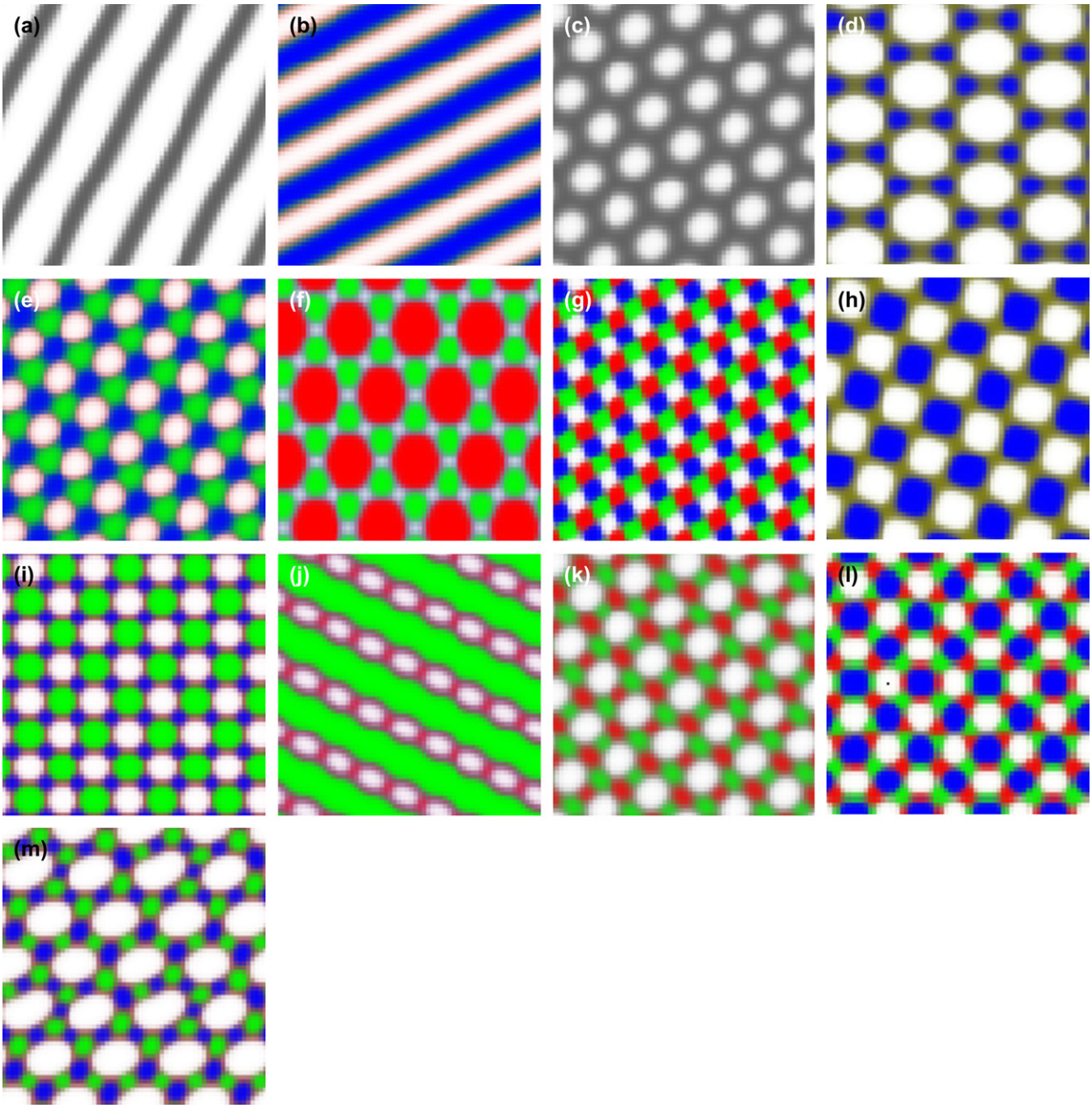

Fig. 1. Ordered microphases of ABCD 4-miktoarm block copolymer with symmetrical interaction parameters $\chi_{AB}N = \chi_{AC}N = \chi_{AD}N = \chi_{BC}N = \chi_{BD}N = \chi_{CD}N$. (a) "Two-color" lamellar phase (LAM_2), (b) "three-color" lamellar phase (LAM_3), (c) hexagonal lattice (HEX), (d) hexagon outside hexagonal lattice (HEX_2), (e) "three-color" hexagonal lattice (HEX_3), (f) hexagon outside "two-color" hexagonal lattice (HEX_{3i}), (g) "four-color" hexagonal lattice (HEX_4), (h) two interpenetrating tetragonal lattice (TET_2), (i) three interpenetrating tetragonal lattice (TET_3), (j) "two-color" lamellae with beads inside ($LAM_2 + BD_i$), (k) hexagon with two interpenetrating tetragonal lattice ($HEX + TET_2$), (l) four interpenetrating tetragonal lattice (TET_4), and (m) hexagonal lattice with two interpenetrating pentagonal lattice ($HEX + PEP_2$). Red, green, blue, and white phases correspond to blocks A, B, C, and D, respectively. (For interpretation of the references to color in this figure legend, the reader is referred to the web version of this article.)

microphase-separated structures—LAM_2, LAM_3, HEX, HEX_2, HEX_3, TET_2, TET_3 and $HEX + TET_2$.

When the repulsive interaction between different blocks is strong, $\tilde{\chi} = 45$, it is more probable for different blocks to separate from each other. The phases turn up various formations at different interaction parameters. When $\tilde{\chi}$ changes from 30 to 45, some new phases occur, such as HEX_{3i}, HEX_4, TET_4, $HEX + PEP_2$ and $LAM_2 + BD_i$. So we can find some interesting morphological changes between different interaction parameters. When $f_A = 0.1, f_B = 0.1, f_C = 0.1$, the phase would change from HEX to LAM_2; when $f_A = 0.1$, $f_B = 0.15$, $f_C = 0.25$, the phase would change from LAM_3 to HEX_{3i}; when $f_A = 0.1$, $f_B = 0.15$, $f_C = 0.3$, the phase would change from LAM_3 to TET_3; when $f_A = 0.15$, $f_B = 0.15$, $f_C = 0.2$,

Table 1
Morphology and saddle-point free energy at different compositions for symmetrical interaction parameters

$f_A/f_B/f_C/f_D$	$\tilde{\chi} = 30$		$\tilde{\chi} = 45$	
	Morphology	Saddle-point free energy	Morphology	Saddle-point free energy
0.1/0.1/0.1/0.7	HEX	7.097395	LAM_2	9.806732
0.1/0.1/0.15/0.65	LAM_3	7.730215	LAM_3	10.438572
0.1/0.1/0.2/0.6	LAM_3	8.188040	LAM_3	10.847588
0.1/0.1/0.25/0.55	LAM_3	8.438473	LAM_3	11.023167
0.1/0.1/0.3/0.5	LAM_3	8.564583	LAM_3	11.087851
0.1/0.1/0.35/0.45	LAM_3	8.624958	LAM_3	11.120432
0.1/0.1/0.4/0.4	LAM_3	8.639929	LAM_3	11.126013
0.1/0.15/0.15/0.6	LAM_2	8.363917	LAM_2	11.457632
0.1/0.15/0.2/0.55	LAM_2	8.946400	$LAM_2 + BDi$	11.869317
0.1/0.15/0.25/0.5	LAM_3	9.182301	HEX_{3i}	12.137703
0.1/0.15/0.3/0.45	LAM_3	9.376822	TET_3	12.318090
0.1/0.15/0.35/0.4	LAM_3	9.438423	TET_3	12.311077
0.1/0.2/0.2/0.5	LAM_2	9.395298	HEX_3	12.491985
0.1/0.2/0.25/0.45	HEX_2	9.905399	HEX_3	12.732033
0.1/0.2/0.3/0.4	TET_3	9.947318	TET_3	12.825201
0.25/0.25/0.25/0.25	N/A[b]	–	HEX_4	15.170712
0.1/0.25/0.3/0.35	HEX_3	10.308853	TET_3	13.215944
0.1/0.3/0.3/0.3	HEX_3	10.405138	DIS[a]	–
0.15/0.15/0.15/0.55	LAM_2	9.013487	LAM_3	12.361471
0.15/0.15/0.2/0.5	LAM_3	9.530403	HEX_2	12.935643
0.15/0.15/0.25/0.45	HEX_2	9.902636	HEX_2	13.154533
0.15/0.15/0.3/0.4	TET_2	10.078515	TET_2	13.288416
0.15/0.15/0.35/0.35	TET_2	10.107382	TET_2	13.281576
0.15/0.2/0.2/0.45	HEX	10.171948	$HEX + PEP_2$	13.690650
0.15/0.2/0.25/0.4	HEX	10.428189	$HEX + PEP_2$	13.936685
0.15/0.2/0.3/0.35	TET_3	10.603147	TET_3	13.962326
0.15/0.25/0.25/0.35	$HEX + TET_2$	10.819948	HEX_3	14.140801
0.15/0.25/0.3/0.3	HEX_3	10.958089	HEX_3	14.257247
0.2/0.2/0.3/0.3	HEX_2	11.087280	TET_4	14.810825
0.1/0.2/0.35/0.35	TET_3	10.064510	TET_3	12.785913
0.1/0.25/0.25/0.4	$HEX + TET_2$	10.167274	HEX_{3i}	13.030159

[a] DIS represents the disordered phase, although this morphology appears to be as HEX_3, there is always flaw on it, so it is supposed to be unstable, so we consider it as DIS.
[b] N/A means that we cannot get a stable morphology of this system.

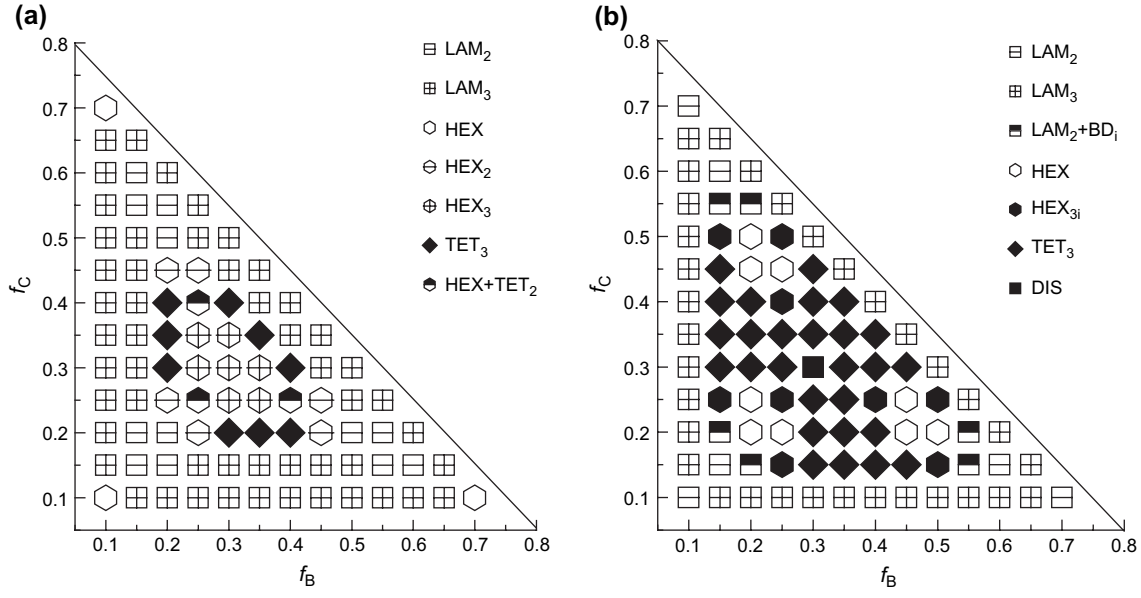

Fig. 2. Microphase diagrams for $f_A = 0.1$ at (a) $\tilde{\chi} = 30$ and (b) $\tilde{\chi} = 45$.

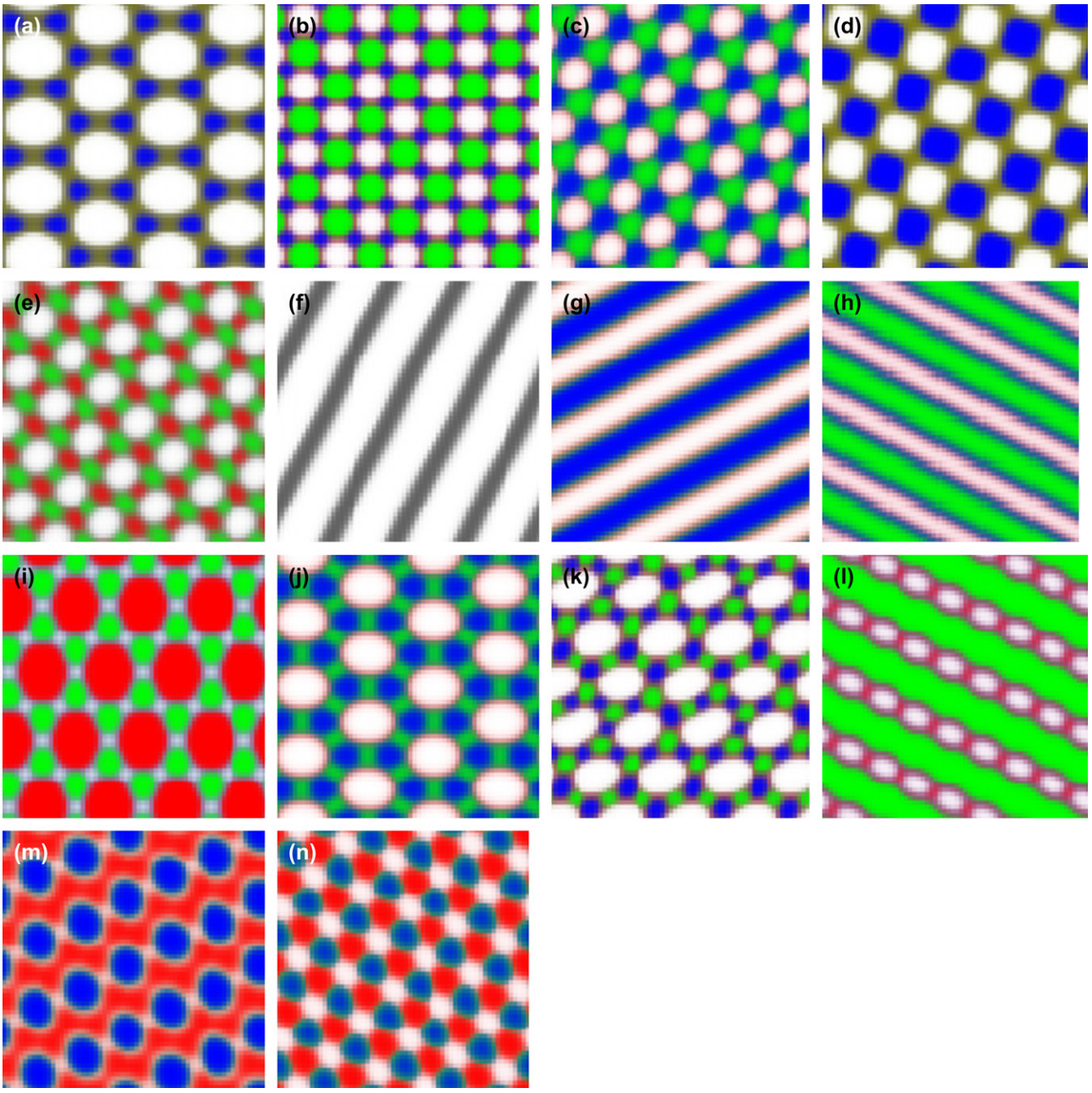

Fig. 3. Ordered microphases of ABCD 4-miktoarm block copolymer with symmetrical interaction parameters $\chi_{AB}N = \chi_{CD}N = 40$, $\chi_{AC}N = \chi_{BD}N = 60$, $\chi_{AD}N = \chi_{BC}N = 20$. (a) HEX_2, (b) TET_3, (c) HEX_3, (d) TET_2, (e) HEX + TET_2, (f) LAM_2, (g) LAM_3, (h) LAM_4, (i) HEX_{3i}, (j) HEX_{3i}*, (k) HEX + PEP_2, (l) LAM_2 + BDi, (m) LAM + BD, and (n) HEX_3 + BD. Red, green, blue, and white phases correspond to blocks A, B, C, and D, respectively. (For interpretation of the references to color in this figure legend, the reader is referred to the web version of this article.)

the phase would change from LAM_3 to HEX_2; when $f_A = 0.1$, $f_B = 0.15$, $f_C = 0.2$, the phase would change from LAM_2 to HEX + TET_2, etc. The morphologies become more complex as the interaction strength increases.

No matter what the interaction parameter is, when three of the four blocks are small enough, for example, $f_A = f_B = f_C = 0.1$, LAM_2 occurs. It is mostly because that the indiscriminate fractions dissolve in each other in one phase and with the rest fraction in another phase. As the composition of any one of the three blocks—take f_C for example, increases, the ordered phase of the polymer changes from LAM_2 to LAM_3 until the increasing block f_C takes the same proportion as f_D does. If the four blocks take an equal proportion, the ordered phase comes up only when the interaction parameter $\tilde{\chi}$ is large enough (in our calculation, when $\tilde{\chi} = 30$, there are no stable phases turn up, when $\tilde{\chi}$ increases to 45, the HEX_4 occurs, which is different from the linear ABCD tetrablock copolymer where LAM_4 emerges). It is hard to separate into different phases when the repulsive interactions between the different blocks are weak for the four comparable

Table 2
Morphology and saddle-point free energy at different compositions for asymmetrical interaction parameters at $\chi_{AB}N = \chi_{CD}N = 40$, $\chi_{AC}N = \chi_{BD}N = 60$, $\chi_{AD}N = \chi_{BC}N = 20$

$f_A/f_B/f_C/f_D$	Morphology	Saddle-point free energy	$f_A/f_B/f_C/f_D$	Morphology	Saddle-point free energy
0.1/0.2/0.3/0.4	HEX_{3i}*	11.067110	0.1/0.1/0.1/0.7	LAM_2	8.692654
0.1/0/2/0.4/0.3	TET_3	11.259151	0.1/0.1/0.7/0.1	LAM_2	8.842301
0.1/0.3/0.2/0.4	HEX_2	11.032558	0.1/0.7/0.1/0.1	LAM_2	8.850747
0.1/0.3/0.3/0.2	HEX_3	11.597126	0.15/0.2/0.3/0.35	LAM_4	11.748886
0.1/0.4/0.2/0.3	TET_2	11.125711	0.15/0.2/0.3/0.35	LAM_4	11.782209
0.1/0.4/0.3/0.2	$HEX + TET_2$	11.587404	0.15/0.3/0.2/0.35	LAM_4	11.770786
0.2/0.1/0.3/0.4	TET_3	11.254353	0.15/0.3/0.35/0.2	HEX_3	12.193354
0.2/0.1/0.4/0.3	HEX_2	11.083847	0.15/0.35/0.2/0.3	LAM_4	11.791052
0.2/0.4/0.1/0.3	HEX_2	11.017488	0.2/0.15/0.3/0.35	LAM_3	11.819828
0.3/0.1/0.2/0.4	HEX_3	11.595352	0.2/0.3/0.35/0.15	$HEX_3 + BD$	12.275918
0.3/0.1/0.4/0.2	HEX_{3i}	11.017931	0.2/0.35/0.3/0.15	$HEX_3 + BD$	12.276084
0.3/0.2/0.1/0.4	$HEX + TET_2$	11.546007	0.3/0.15/0.2/0.35	$HEX_3 + BD$	12.153390
0.3/0.2/0.4/0.1	$LAM_2 + BD$	11.142467	0.3/015/0.35/0.2	LAM_3	11.904766
0.3/0.4/0.2/0.1	TET_3	11.346863	0.3/0.2/0.35/0.15	LAM_3	11.952467
0.3/0.4/0.1/0.2	HEX_{3i}	11.237955	0.3/0.35/0.2/0.15	LAM_4	11.954596
0.4/0.1/0.3/0.2	$LAM + BD$	11.152053	0.35/0.15/0.2/0.3	$HEX_3 + BD$	12.152288
0.4/0.2/0.1/0.3	HEX_3	11.587412	0.35/0.3/0.2/0.15	LAM_3	11.789424
0.4/0.2/0.3/0.1	HEX_{3i}	11.028189	0.1/0.1/0.4/0.4	LAM_3	9.838690
0.4/0.3/0.1/0.2	TET_3	11.344181	0.1/0.15/0.15/0.6	LAM_3	9.762609
0.4/0.3/0.2/0.1	HEX_{3i}	11.085870	0.1/0.15/0.25/0.5	LAM_3	10.386135
0.1/0.15/0.60/0.15	LAM_3	10.054401	0.1/0.2/0.2/0.5	LAM_3	10.668264
0.1/0.2/0.35/0.35	TET_3	11.196762	0.1/0.25/0.15/0.5	LAM_4	10.266657
0.1/0.25/0.25/0.4	HEX_{3i}	11.235428	0.1/0.25/0.3/0.35	HEX_{3i}*	11.409134
0.1/0.3/0.25/0.35	HEX_{3i}	11.393382	0.1/0.3/0.3/0.3	HEX_3	11.608790
0.1/0.3/0.35/0.25	HEX_3	11.627037	0.1/0.35/0.25/0.3	TET_3	11.460629
0.1/0.35/0.3/0.25	HEX_3	11.576147	0.1/0.4/0.25/0.25	TET_3	11.425741
0.1/0.4/0.4/0.1	TET_3	10.736036	0.1/0.5/0.15/0.25	LAM_4	10.340479
0.1/0.5/0.2/0.2	LAM_3	10.852685	0.1/0.5/0.25/0.15	$LAM_2 + BD_i$	11.029345
0.1/0.6/0.15/0.15	LAM_3	9.924255	0.1/0.1/0.15/0.65	LAM_3	9.251562
0.1/0.1/0.25/0.55	LAM_3	9.732704	0.1/0.1/0.3/0.5	LAM_3	9.799735
0.1/0.1/0.35/0.45	LAM_3	9.828619	0.1/0.1/0.45/0.35	LAM_3	9.832630
0.1/0.1/0.5/0.3	LAM_3	9.798769	0.1/0.1/0.55/025	LAM_3	9.728432
0.1/0.15/0.1/0.65	LAM_3	9.157048	0.1/0.15/0.2/0.55	LAM_3	10.155350
0.1/0.15/0.3/0.45	LAM_3	10.488654	0.1/0.15/0.35/0.4	LAM_3	10.532043
0.1/0.15/0.4/0.35	LAM_3	10.559833	0.1/0.15/0.45/0.3	LAM_3	10.551234
0.1/0.15/0.5/0.25	LAM_3	10.488739	0.1/0.15/0.55/0.2	LAM_3	10.383835
0.1/0.2/0.15/0.55	LAM_3	10.073819	0.1/0.2/0.25/0.45	LAM_3	10.940494
0.1/0.2/0.45/0.25	TET_3	11.137117	0.1/0.2/0.5/0.2	$LAM_2 + BD_i$	11.007996
0.1/0.2/0.55/0.15	$LAM_2 + BD_i$	10.676329	0.1/0.25/0.2/0.45	LAM_3	10.916889
0.1/0.25/0.35/0.3	TET_3	11.473969	0.1/0.25/0.4/0.25	TET_3	11.514345
0.1/0.25/0.45/0.2	TET_3	11.471892	0.1/0.25/0.5/0.15	$LAM_2 + BD_i$	11.072787
0.1/0.25/0.55/0.1	$LAM_2 + BD_i$	10.357113	0.1/0.3/0.15/0.45	LAM_3	10.354010
0.1/0.3/0.3/0.3	HEX_3	11.608790	0.1/0.3/0.4/0.2	HEX_3	11.581747
0.1/0.3/0.5/0.1	HEX_{3i}	10.570357	0.1/0.35/0.2/0.35	HEX_2	11.153364
0.1/0.35/0.35/0.2	HEX_3	11.558952	0.1/0.35/0.4/0.15	HEX_3	11.421067
0.1/0.4/0.15/0.35	LAM_3	10.413633	0.1/0.4/0.35/0.15	HEX_3	11.428080
0.1/0.45/0.15/0.3	LAM_3	10.401572	0.1/0.45/0.3/0.15	$HEX + PEP_2$	11.326962
0.1/0.45/0.25/0.2	TET_3	11.361839	0.1/0.45/0.2/0.25	LAM_4	11.015997
0.1/0.45/0.35/0.1	TET_3	11.003225	0.1/0.55/0.2/0.15	LAM_3	10.578413
0.1/0.55/0.15/0.2	LAM_3	10.193525	0.1/0.6/0.15/0.15	LAM_3	9.924255
0.1/0.55/0.25/0.1	$LAM_2 + BD_i$	10.366969	0.1/0.1/0.6/0.2	LAM_3	9.568447
0.1/0.6/0.2/0.1	$LAM_2 + BD_i$	10.135798	0.1/0.1/0.2/0.6	LAM_3	9.567633
0.1/0.2/0.6/0.1	$LAM_2 + BD_i$	9.984068	0.1/0.15/0.65/0.1	LAM_3	9.575206
0.1/0.1/0.65/0.15	LAM_3	9.396376	0.1/0.25/0.1/0.55	LAM_3	9.539185
0.1/0.2/0.1/0.6	LAM_3	9.413677	0.1/0.35/0.1/0.45	LAM_3	9.628210
0.1/0.3/0.1/0.5	LAM_3	9.603250	0.1/0.35/0.2/0.35	HEX_2	11.062231
0.1/0.35/0.15/0.4	LAM_3	10.393357	0.1/0.45/0.1/0.35	LAM_3	9.637491
0.1/0.4/0.1/0.4	LAM_3	9.642411	0.1/0.5/0.3/0.1	$HEX + PEP_2$	11.333887
0.1/0.5/0.1/0.3	LAM_3	9.603305	0.1/0.6/0.1/0.2	LAM_3	9.403621
0.1/0.55/0.1/0.25	LAM_3	9.539237	0.1/0.65/0.15/0.1	LAM_3	9.554197
0.1/0.65/0.1/0.15	LAM_3	9.229463	0.1/0.35/0.45/0.1	$HEX + PEP_2$	11.003942

compositions. And it is obvious that systems with similar compositions have similar morphologies no matter the interaction parameter is large or small.

By using the above computational results, we can obtain the microphase diagrams at small fractions of one of the blocks, such as f_A, at $\tilde{\chi} = 30$ and 45 as shown in Fig. 2.

Since the interaction parameters are symmetrical, we can easily conclude that if we change the positions of A, B, C, or D without changing their volume fractions, the morphologies will stay the same as the original. That is to say we can change the position of B, C and D randomly. That is why the phases in Fig. 2 have such a high symmetry. But when it comes to the linear copolymers, situations change [28]. There are many different morphologies like LAM_4 (''four-color lamellae''), CSH (core–shell hexagonal lattice), CST_2 (core–shell two interpenetrating tetragonal lattice), LAM + BD (lamellae with beads inside), CS_3H (''three-color'' core–shell hexagonal phase), LAM + BD_2 (lamellae with ''two-color'' beads inside). Meanwhile, many morphologies occurred in the present case disappear, such as, HEX, HEX_2, HEX_3, HEX_{3i}, TET_2, TET_3, TET_4, HEX + PEP_2, and HEX + TET_2. That shows that the morphology not only depends on the composition of the block copolymer but also relies on its architecture [28].

When the morphologies and the phase diagrams are compared with the star ABC triblock copolymer [3], the phase behaviors show some similarity, but one more phase occurs due to an additional block. Let us take $f_A = 0.1$ at $\tilde{\chi} = 30$ as an example. When one of the blocks is very small, such as $f_i = 0.1$ (i = A, B, C, or D), the stable morphology is hexagonal phase (HEX). But when the composition of one block increases, the lamellae phase occurs. With the compositions of the two blocks increasing further, the stable ordered phase changes from HEX → HEX + TET_2 → HEX_3 → TET_3. When the compositions of the three blocks are comparable, the HEX_3 is stable.

3.2. Asymmetrical interaction parameters

If we change the symmetry of the interaction parameters, the morphologies of the system would be more complex. There exists permutation symmetry (A–B, A–C, A–D, B–C, B–D, C–D) of the four blocks at the symmetrical interaction parameters, i.e., the microphase will not be altered by the sequence of the blocks. When $f_i = 0.1$, $f_j = 0.2$, $f_k = 0.3$, $f_l = 1 - f_i - f_j - f_k = 0.4$ (ijkl = ABCD or its compositions with difference sequences), the stable phase is three alternating tetragonal lattice.

But when we change the interaction parameters to $\chi_{AB}N = \chi_{CD}N = 40$, $\chi_{AC}N = \chi_{BD}N = 60$, $\chi_{AD}N = \chi_{BC}N = 20$, as ijkl take different numerical values of 0.1, 0.2, 0.3 and 0.4 randomly, the phases vary as well. Fig. 3 shows the morphologies of ABCD 4-miktoarm star block copolymer at $\chi_{AB}N = \chi_{CD}N = 40$, $\chi_{AC}N = \chi_{BD}N = 60$, $\chi_{AD}N = \chi_{BC}N = 20$. We found 14 microphases in this case. Compared with the case for the symmetric interaction parameters, the new phases occur, such as LAM_4, HEX_{3i}*, LAM + BD, and HEX_3 + BD.

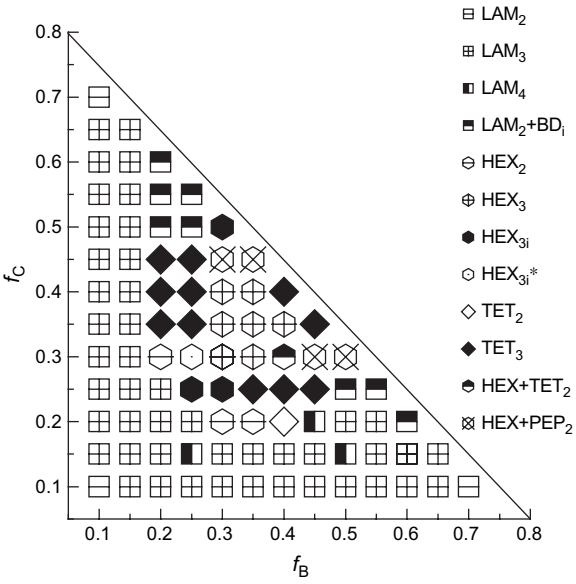

Fig. 4. The microphase diagram for $f_A = 0.1$ at $\chi_{AB}N = \chi_{CD}N = 40$, $\chi_{AC}N = \chi_{BD}N = 60$, $\chi_{AD}N = \chi_{BC}N = 20$.

The morphologies and saddle-point free energies at different compositions for asymmetrical interaction parameters are listed in Table 2. Based on the phases above, the microphase diagram is constructed as shown in Fig. 4.

It is clear that although the symmetry of interaction parameters is reduced, the discipline we conclude before still fit the situation. Systems with similar compositions have similar morphologies. But we cannot randomly change the position of the arms if we want to get the same morphology as the original one. From Fig. 4 we can see that if we change the position of the arms of the copolymer, we may get different morphologies. It is the difference among interaction parameters that influences the morphology of the system. We also find that there are still some morphologies with same occurrence when we change the position of the arms. This is not strange because we did not suppose all the interaction parameters are different from each other. It is due to the low symmetry of interaction parameters that the phenomenon occurs.

4. Conclusions

By using the implementation of the self-consistent field theory (SCFT), the ABCD 4-miktoarm block copolymers are investigated in two-dimensional demonstration. The morphologies and the phase diagrams are intensively presented.

The stable ordered morphologies of the ABCD type not only depend on the composition, but also on the segregation degree. No matter what the interaction parameters are, systems with similar composition have similar morphologies at the symmetrical interaction parameters, i.e., $\chi_{AB}N = \chi_{AC}N = \chi_{AD}N = \chi_{BC}N = \chi_{BD}N = \chi_{CD}N = \tilde{\chi}$. At the weaker segregation, such as $\tilde{\chi} = 30$, the minority component always cannot separate from the adjacent block and dissolve to form one phase with the adjacent block. That is why LAM_n ($n = 2$, 3)

always turn up. With the increase of the segregation degree, such as $\tilde{\chi} = 45$, the ordered phases are well separated, and many new morphologies come up, such as HEX_{3i}, HEX_4, TET_4, $HEX + PEP_2$ and $LAM_2 + BD_i$.

When $\chi_{AB}N = \chi_{CD}N = 40$, $\chi_{AC}N = \chi_{BD}N = 60$, $\chi_{AD}N = \chi_{BC}N = 20$, the morphologies become more complex compared with the case for the symmetrical interaction parameters. Many interesting patterns occur, like LAM_4, HEX_{3i}*, LAM + BD, and HEX_3 + BD. The above results are helpful in designing new nanomaterial involving ABCD 4-mitoarm star block copolymers.

Acknowledgement

This work has been supported by National Natural Science Foundations of China (Nos. 20674035, 20504013 and 50533020), Nanjing University Talent Development Foundation (No. 0205004107) and Natural Science Foundation of Nanjing University (No. 0205005216).

References

[1] Matsen MW, Schick M. Physical Review Letters 1994;72:2660.
[2] Tang P, Qiu F, Zhang HD, Yang YL. Physical Review E 2004;69:031803.
[3] Tang P, Qiu F, Zhang HD, Yang YL. Journal of Physical Chemistry B 2004;108:8434–8.
[4] He XH, Song M, Liang HJ, Pan CY. Journal of Chemical Physics 2001;114:10510.
[5] He XH, Huang L, Liang HJ, Pan CY. Journal of Chemical Physics 2002;116:10508.
[6] Gemma T, Hatano A, Dotera T. Macromolecules 2002;35:3225.
[7] Nakazawa H, Ohta T. Macromolecules 1993;26:5503.
[8] Mogi Y, Kotsuji H, Kaneko T, Mori K, Matsushita Y, Noda I. Macromolecules 1992;25:5408.
[9] Mogi Y, Mori K, Kotsuji H, Matsushita Y, Noda I. Macromolecules 1993;26:5169.
[10] Mogi Y, Mori K, Matsushita Y, Noda I. Macromolecules 1992;25:5412.
[11] Mogi Y, Nomura M, Kotsuji H, Ohnishi K, Matsushita Y, Noda I. Macromolecules 1994;27:6755.
[12] Jung K, Abetz V, Stadler R. Macromolecules 1996;29:1076.
[13] Lyatskaya YV, Birshtein TM. Polymer 1995;36:975.
[14] Stadler R, Auschra C, Beckmann J, Krappe U, Voit-Martin I, Leibler L. Macromolecules 1995;28:3080.
[15] Bates FS, Fredrickson GH. Physics Today 1999;52:32.
[16] Matsushita Y. Macromolecules 2007;40:771–6.
[17] Takano A, Soga K, Suzuki J, Matsushita Y. Macromolecules 2003; 36:9288.
[18] Takahashi K, Hasegawa H, Hashimoto T, Bellas V, Iatrou H, Hadjichristidis N. Macromolecules 2002;35:4859.
[19] Takano A, Soga K, Asari T, Suzuki J, Arai S, Saka H, et al. Macromolecules 2003;36:8216.
[20] Ekizoglou N, Hadjichristidis N. Journal of Polymer Science, Part A: Polymer Chemistry 2002;40:2166.
[21] Li Z, Liu GJ. Langmuir 2003;19:10480.
[22] Fragouli PG, Iatrou H, Hadjichristidis N. Journal of Polymer Science, Part A: Polymer Chemistry 2003;42:514.
[23] Iatrou H, Hadjichristidis N. Macromolecules 1993;26:2479.
[24] Dotera T. Physical Review Letters 1999;82:105.
[25] Dotera T, Hatano A, Gemma T. Kobunshi Ronbunshu 1999;56:667.
[26] Drolet F, Fredrickson GH. Macromolecules 2001;34:5317.
[27] Drolet F, Fredrickson GH. Physical Review Letters 1999;83:4317.
[28] Wang R, Hu JL, Jiang ZB, Zhou DS. Macromolecular Theory and Simulations 2005;14:256.
[29] Hasegawa H, Takahashi K, Hashimoto T, Iatrou H, Bellas V, Hadjichristidis N. Abstracts of Papers of the American Chemical Society 2003;225:U675.
[30] Hadjichristidis N. Journal of Polymer Science, Part A: Polymer Chemistry 1999;37:857.
[31] Ruokolainen J, Saariaho M, Ikkala O, ten Brinke G, Thomas EL, Torkkeli M, et al. Macromolecules 1998;32:1152.
[32] Ruokolainen J, Makinen R, Torkkeli M, Makela T, Serimaa R, ten Brinke G, et al. Science 1998;280:557.
[33] Ruokolainen J, ten Brinke G, Ikkala O. Advanced Materials 1999;11:777.
[34] Saito R, Fujita A, Ichimura A, Ishizu K. Journal of Polymer Science, Polymer Chemistry Edition 2000;38:2091.